Autoreduction of Cyanoferrate(III) Ions in a Polymer Electrolyte Membrane: All Solid State Electrochemical and Spectroscopic Investigations

Meera Parthasarathy,[†] Chinnakonda S. Gopinath,[‡] and Vijayamohanan K. Pillai*[,†]

Physical and Materials Chemistry Division and Catalysis Division, National Chemical Laboratory, Pune, Maharashtra, India 411 008

Received June 21, 2006. Revised Manuscript Received August 25, 2006

The effect of dielectric confinement on proton-coupled electron-transfer behavior and spectroscopic properties of cyanoferrate ions in a polymer electrolyte membrane (Nafion) has been investigated in an "all-solid-state" electrochemical cell, using techniques such as cyclic voltammetry, zero current chronopotentiometry, electrochemical impedance, diffuse reflectance infrared Fourier transform spectroscopy (DRIFT), UV−visible spectroscopy, X-ray photoelectron spectroscopy (XPS), and electron spin resonance spectroscopy (ESR). From the above investigations, we found that cyanoferrate(III) ions undergo autoreduction in the ionomer matrix, for which a sulfonate-coupled mechanism has been proposed. This report demonstrates the effectiveness of the micellar interface in tuning the redox potential of the confined ions. A systematic analysis of the cyclic voltammetry and impedance data for the $[Fe(CN)_6]^{4-}$-containing Nafion membrane enables the estimation of a standard rate constant for $[Fe(CN)_6]^{4-}$ oxidation, k^o, as 5.44×10^{-6} cm/s and a diffusion coefficient, D_o, as 1.3×10^{-12} cm^2/s. A similar calculation yields a value of 4.8×10^{-12} cm^2/s for the diffusion coefficient of protons and 9.1×10^{-6} cm/s for the standard rate constant for hydrogen oxidation. The similarity in mass-transfer coefficients calculated for protons and $[Fe(CN)_6]^{4-}$ ions suggests a proton-coupled electron-transfer mechanism for the $[Fe(CN)_6]^{4-}/[Fe(CN)_6]^{3-}$ couple. The results of the above investigations could have direct technological relevance for deciding catalyst materials having redox compatibility with the polymer electrolyte, especially in the preparation of catalyst-coated membranes (wherein the fuel-cell catalyst is directly coated onto the polymer membrane instead of on the carbon support).

1. Introduction

Ion-exchange resins form an important class of materials because of their increasing demand as solid electrolytes in modern energy generation and storage devices, such as fuel cells and supercapacitors, respectively, in addition to their conventional applications in analytical separation techniques. Being a panacea for a wide range of technologies, polymer electrolyte research is one of the major areas of current interest and is being carried out from different perspectives. One such perspective in polymer electrolyte research is the study of dynamics and energetics of ionic species incorporated in such solid electrolytes,[1] with the primary motivation being to understand the effect of confinement in the micellar environment offered by the ionic polymer on properties of incorporated species. Among the various polymer electrolytes, Nafion (a poly(tetrafluoroethylene)-based ionomer), developed by DuPont de Nemours & Co., is the most widely employed material, mainly because of its high proton conductivity. A fairly recent review by Mauritz and Moore gives an extensive account of experimental and theoretical investigations carried out with Nafion.[2] In this regard, a number of reports exist on the study of the nature of ion fluxes in Nafion membranes using scanning electrochemical microscopy,[3−7] the effect of surfactants on the ion fluxes,[8,9] and the local structure around incorporated ions in the ionomers using techniques such as EXAFS,[10] Raman spectroscopy,[11] NMR,[12] and ESR.[13−17] Also, the environmental changes in chromophore entities incorporated in the matrix

* Corresponding author. E-mail: vk.pillai@ncl.res.in. Phone: 91-020-25902270. Fax: 91-020-25902636.
[†] Physical and Materials Chemistry Division, National Chemical Laboratory.
[‡] Catalysis Division, National Chemistry Laboratory.

(1) Alonso-Amigo, M. G.; Schlick, S. *J. Phys. Chem.* **1986**, *90*, 6353−6358.
(2) Mauritz, K. A.; Moore, R. B. *Chem. Rev.* **2004**, *104*, 4535−4585.
(3) Gyurcsanyi, R. E.; Pergel, E.; Nagy, R.; Kapui, I.; Lan, B. T. T.; Toth, K.; Bitter, I.; Linder, E. *Anal. Chem.* **2001**, *73*, 2104−2111.
(4) Lee, C.; Anson, F. C. *Anal. Chem.* **1992**, *64*, 528−533.
(5) Nugues, S.; Denuault, G. *J. Electroanal. Chem.* **1996**, *408*, 125−140.
(6) Jeon, C.; Anson, F. C. *Anal. Chem.* **1982**, *84*,2021−2028.
(7) Kwak, J.; Anson, F. C. *Anal. Chem.* **1992**, *6664*, 250−256.
(8) Moore, C. M.; Hackman, S.; Brennan, T.; Minteer, S. D. *J. Membr. Sci.* **2005**, *255*, 233−238.
(9) Moore, C. M.; Hackman, S.; Brennan, T.; Minteer, S. D. *J. Membr. Sci.* **2005**, *254*, 63−70.
(10) Pan, H. K.; Meagher, A.; Pineri, M.; Knapp, G. S.; Cooper, S. L. *J. Chem. Phys.* **1985**, *82*, 1529
(11) Neppel, A.; Butler, I. S.; Eisenberg, A. *Macromolecules* **1979**, *12*, 948
(12) Schlick, S.; Gobel, G.; Pineri, M; Volino, F. *Macromolecules* **1991**, *24*, 3517−3521
(13) Rex, G. C.; Schlick, S. *J. Phys. Chem.* **1985**, *89*, 3598−3601.
(14) Alonso-Amigo, M. G .; Schlick, S. *J. Phys. Chem.* **1989**, *93*, 7526−7528.
(15) Bednarek, J.; Schlick, S. *J. Am. Chem. Soc.* **1990**, *112*, 5019−5024.
(16) Bednarek, J.; Schlick, S. *J. Am. Chem. Soc.* **1991**, *113*, 3303−3309.
(17) Maiti, B.; Schlick, S. *Chem. Mater.* **1992**, *4*, 458−462.

10.1021/cm061444i CCC: $33.50
Published on Web 10/11/2006

have been probed by observing solvatochromic shifts.[18] In all these cases, the usual approach has been to incorporate ions having a charge opposite to that of the pendent groups in the polymer chain. In this paper, we report a novel strategy, the incorporated ion probe approach, in which anionic complexes (cyanoferrate(II) and cyanoferrate(III)) incorporated in an anionic polymer matrix (Nafion) act as probes, providing information about the local structure of the membrane as a function of the applied electric field. Because a negatively charged interface (formed by sulfonate groups in Nafion) can confine a negative ion more effectively (because of electrostatic repulsion) to certain regions than a positive ion, this protocol could be more appropriate for studying the effect of confinement in the polymer matrix on the charge-transfer behavior of redox species. However, this expectation is primarily based on electrostatic considerations, although hydrophobic and Van der Waals interactions also play a dynamic role in facilitating ion transport in the polymer membrane.

Nevertheless, studying the charge-transfer kinetics and thermodynamics of anions in an anionic matrix gives useful information about the nature of the interface between hydrophilic and hydrophobic domains, which plays an important role in proton transport when the membrane is used as an electrolyte in a polymer electrolyte membrane fuel cell (PEMFC). The long-term performance of the polymer-electrolyte-based energy devices depends critically on the compatibility and stability of the ion-exchange membrane under the desired operating conditions of the device. Hence an understanding of the multifunctional behavior of the membranes and structure−property correlation at the microscopic level would help improve the performance of the devices that incorporate the membranes. However, a real time analysis of the membrane incorporated in a fuel cell is unlikely because of various other contributions from both dynamic and static variables, such as field, humidity, concentration, and thermal gradients controlling the overall device performance. To circumvent this difficulty, it has been a common practice to study the electrochemical behavior of electrodes coated with the polymer film dipped in a liquid electrolyte, facilitating the extrapolation of the results to the real device conditions.[19,20] In this protocol, a contribution from the interface between the solid membrane and the liquid electrolyte is unavoidable. A more relevant approach is to study the membrane in an all-solid-state configuration; in this regard, few preliminary reports are available with different solid electrolytes.[21−23,40]

In this paper, we report our electrochemical and spectroscopic investigations of Nafion membranes containing cyanoferrate ions, using an all-solid-state configuration. The results demonstrate the effect of an abrupt change in the dielectric constant (for example, Paddison et al. have reported the variation of permittivity with radial distance from the pore wall in Nafion for $\lambda = 22.5$ using statistical mechanics[24]) and hence the local electric field[25,26] at the micellar interface between the hydrophobic and hydrophilic domains (∼10−50 Å in dimension[27]) in the polymer on the stability of the incorporated ions (which could be broadly called the dielectric confinement effect) compared to earlier reports in Nafion on the effect of hydrophobic confinement on the transport properties of the membrane.[27,28] In addition, the present investigations on chemically modified electrolytes add another dimension to the tunability of device performance along with the usual strategy of chemically modified electrodes. Moreover, the coupling of proton transfer with the outersphere electron-transfer capability of the confined redox couple has direct significance for optimizing the design of catalyst-coated membranes for applications in fuel cells, supercapacitors, solid-state hydrogen sensors, and analytical techniques based on ion-exchange membranes.

2. Experimental Section

2.1. Materials. A 5 wt % solution of Nafion in a mixture of lower aliphatic alcohols and water (eq wt 1000) was procured from Aldrich Chemicals, and potassium ferrocyanide trihydrate and potassium ferricyanide were procured from Qualigens Fine Chemicals, Mumbai, India. Deionized water (Millipore 18 MΩ) was used for preparing the cyanoferrate solutions.

2.2. Methods. *Electrochemistry.* All-solid-state cyclic voltammetry was carried out using a specially designed homemade electrochemical cell made of Teflon, shown in Scheme 1. The cell consisted of a cylindrical block of Teflon 1.7 cm in height and 0.8 cm in diameter. At one end of the block, a shallow trough 1 mm in depth was made. For housing the electrodes, we drilled three holes through the center of the trough to the other end of the cylinder at appropriate positions such that the counter electrode (a 0.5 mm Pt wire) encircles the working (a 0.140 mm Pt wire) and the reference electrodes (Ag/AgCl electrode obtained by chloridation of a 0.5 mm Ag wire) inserted in the middle holes. A provision

(18) Che, C. M.; Fu, W. F.; Lai, S. W.; Hou, Y. J.; Liu, Y. L. *Chem. Commun.* **2003**, 118−119.
(19) Maruyama, J.; Abe, I. *J. Electroanal. Chem.* **2002**, *527*, 65−70.
(20) Kalj, B.; Dryfe, R. A. W. *Phys. Chem. Chem. Phys.* **2001**, *3*, 3156−3164.
(21) Riess, I. *Solid State Ionics* **2005**, *176*, 1667−1674.
(22) Claye, A. S.; Fischer, J. E.; Huffman, C. B.; Rinzler, A. G.; Smalley, R. E. *J. Electrochem. Soc.* **2000**, *147* (8), 2845−2852.
(23) Basura, V. I.; Beattie, P. D.; Holdcroft, S. *J. Electroanal. Chem.* **1998**, *458*, 1−5.
(24) Paul, R.; Paddison, S. J. *Solid State Ionics* **2004**, *168*, 245−248.
(25) Eikerling, M.; Kornyshev, A.; Kuznetsov, A. M.; Ulstrup, J.; Walbran, S. *J. Phys. Chem. B* **2001,** *105*, 3646
(26) Paddison, S. J.; Paul, R.; Zawodzinski, T. A., Jr. *J. Chem. Phys.* **2001**, *115*, 7753
(27) Deng, Z. D.; Mauritz, K. A. *Macromolecules* **1992**, *25*, 2369−2380.
(28) Mauritz, K. A. *Macromolecules* **1989**, *22*, 4483−4488.
(29) Borchert, H.; Talapin, D. V.; Goponik, N.; McGinley, C.; Adam, S.; Lobo, A.; Moller, T.; Weller, H. *J. Phys. Chem. B* **2003**, *107*, 9662.
(30) The spectra were fitted using the software XPSPEAK4.1, which is available free on the Web site www.uksaf.org/software.html#7.
(31) Lu, X.; Wu, S.; Wang, L.; Su, Z. *Sens. Actuators, B* **2005**, *107*, 812−817.
(32) Maruyama, J.; Inaba, M.; Katakura, K.; Ogumi, Z.; Takehara, Z. I. *J. Electroanal. Chem.* **1998**, *447*, 201−209.
(33) Jiang, J.; Kucernak, A. *J. Electroanal. Chem.* **2004**, *567*, 123−137.
(34) Bard, A. J.; Faulkner, L. R. *Electrochemical Methods: Fundamentals and Applications*, 2nd ed.; Wiley: New York, 2004; p 236
(35) Seeliger, D.; Hartnig, C.; Spohr, E. *Electrochim. Acta* **2005**, *50*, 4234−4240.
(36) Paddison, S. J.; Paul, R. *Phys. Chem. Chem. Phys.* **2002**, *4*, 1158−1163.
(37) Eikerling, M.; Kornyshev, A. A. *J. Electroanal. Chem.* **2001**, *502*, 1.
(38) Bard, A. J.; Faulkner, L. R. *Electrochemical Methods: Fundamentals and Applications*, 2nd ed.; Wiley: New York, 2004; p 99.
(39) Liu, Y.; Huang, B.; Tzeng, I. *J. Electroanal. Chem.* **2002**, *533*, 85−90.
(40) Kulesza, P. J.; Dickinson, E. V.; Williams, M. E.; Hendrickson, S. M.; Malik, M. A.; Miecznikowski, K.; Murray, R. W. *J. Phys. Chem. B* **2001**, *105*, 5833−5838.

Scheme 1. Electrochemical Cell for All Solid-State Investigations with Polymer Electrolytes[a]

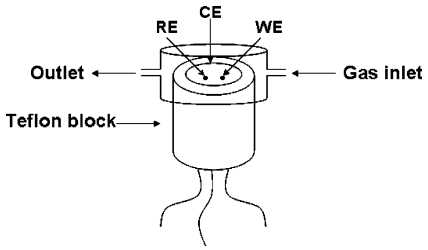

[a] WE, working electrode; CE, counter electrode; RE, reference electrode.

was made for performing the experiments in different gaseous atmospheres by fabricating a two-way screw cap over the cylindrical Teflon block. Cyclic voltammetry with a pristine Nafion membrane was conducted with an Autolab PGSTAT30 (ECO CHEMIE) instrument using a continuous film of Nafion (thickness 0.5 mm), cast over the electrodes fixed in the Teflon cell. A 0.5 M aqueous solution of $K_4[Fe(CN)_6]$ (20 μL) was then added to the membrane to give a final concentration of 6.7×10^{-3} M. Enough time was given for the ions to diffuse through the membrane, and the electrochemical experiments for the ion- incorporated membrane were then performed at room temperature (30 °C). OCV−time profiles were also recorded for Nafion membranes with different concentrations of potassium ferricyanide (683, 1366, and 2732 μM) using the same instrument. Electrochemical impedance studies were performed with the same cell using an Autolab PGSTAT30 (ECO CHEMIE) instrument equipped with a frequency response analyzer immediately after adding equal proportions of $K_4[Fe(CN)_6]$ and $K_3[Fe(CN)_6]$ (3.4×10^{-3} M each) using a 10 mV rms AC signal in the frequency range 10 mHz to 100 kHz.

Spectroscopic Investigations. The Nafion membranes were peeled from the holder after cyclic voltammetry and used for XPS, ESR, UV−visible, and IR spectral investigations. The XPS of $K_3[Fe(CN)_6]$/Nafion (0.05 M) was recorded 1 h after the addition of ferricyanide to the membrane. XPS measurements were carried out on a VG MicroTech ESCA 3000 instrument at a pressure of $>1 \times 10^{-9}$ Torr (pass energy of 50 eV, electron takeoff angle 60°, and overall resolution ~1 eV using a monochromatic Al Kα source ($h\nu = 1486.6$ eV)). The core level spectra of the C 1s, O 1s, N 1s, F 1s, Fe 2p, and S 2p signals were recorded with an overall instrumental resolution of ~1 eV. The alignment of binding energy (BE) was carried out using a C 1s BE of 285 eV as the reference. The X-ray flux (power 70 W) was kept deliberately low to reduce beam-induced damage. The spectra were fitted using a combined polynomial and Shirley type background function.[29,30] ESR spectra were recorded on a Bruker EMX spectrometer operating at X-band frequency (~9.784 Hz). The samples were analyzed at both 298 and 77 K. The UV−visible spectra of the solid membranes were recorded (in the transmittance mode) using a JASCO Model V-570 dual beam spectrophotometer operating at a resolution of 2 nm; the solid-state UV−visible spectra of the potassium ferrocyanide and potassium ferricyanide were recorded (in the reflectance mode) using a Perkin-Elmer Lambda 650 instrument operating at a resolution of 5 nm. For IR spectroscopy, a Perkin-Elmer FTIR Spectrum One spectrophotometer operating in the diffuse reflectance mode at a resolution of 4 cm^{-1} was used. All these studies were repeated for cyanoferrate-incorporated membranes prepared under identical conditions, without subjecting them to an electric field.

3. Results and Discussion

3.1. Electrochemistry. *3.1.1. Cyclic Voltammetry.* Figure 1 shows cyclic voltammograms of the Nafion membrane with and without $K_4[Fe(CN)_6]$ as the polymer electrolyte, using the all-solid-state cell. The open circuit potential (OCV) of the cell using the pristine membrane as the polymer electrolyte is +0.28 V. Subsequently, when the potential is scanned from −0.5 to +0.6 V, at a scan rate of 100 mV/s, no faradaic peaks are observed in the potential window between + 0.596 and −0.500 V, where oxygen and hydrogen evolution occur, respectively. In contrast, the $K_4[Fe(CN)_6]$-incorporated membrane shows an OCV of + 0.164 V, which is more negative (by 116 mV) than that of the pristine membrane. This change in OCV corresponds to a positive shift in the free energy of the reaction by 11.2 kJ/mol, which shows the presence of chemical interactions between the ionomer and the incorporated complex anions. When the potential is scanned between −0.25 and +0.5 V, at a scan rate of 100 mV/s, two anodic peaks, one at −0.003 V (peak a) and another at +0.284 V (peak b) along with a cathodic peak at +0.156 V (peak c) are observed (Figure 1). Peak a could be assigned to the oxidation of adsorbed H_2, because there is an increase in the peak current when the potential is held at −0.25 V for 2 min. This is further confirmed by an increase in the peak current with an increase in the partial pressure of the H_2 gas passing over the membrane (Figure 2). The scaling of peak current with hydrogen partial pressure has implications for solid-state H_2 sensing; a report on all-solid-state hydrogen sensing using a commercial Nafion membrane is available.[31] Voltammograms at different potential scan rates (10, 25, 50, 100, and 200 mV/s) clearly indicate a shift in the peak potential, E_{pa}, to more positive values, as revealed in Figure 3. This is expected, because for an irreversible charge-transfer process, E_p is supposed to be shifted in the positive direction (for an oxidation process) by $1.15RT/\alpha F$ (where R is the gas constant, T is the temperature in K, α is the charge-transfer coefficient and F is the Faraday constant) for every 10-fold increase in the scan rate.[54] In this system, the peak potential shifts by +22

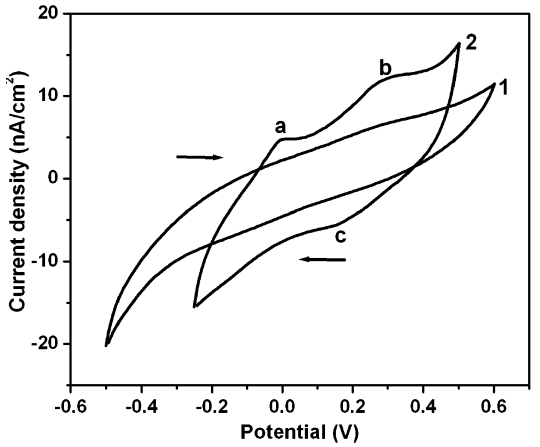

Figure 1. Cyclic voltammograms of (1) the pristine Nafion membrane and (2) the $K_4[Fe(CN)_6]$/Nafion membrane (6.7×10^{-3} M) at a scan rate of 100 mV/s using a Pt disk working electrode (0.14 mm diameter), Ag/AgCl reference, and Pt counter electrode (peak a, H_2 oxidation; peak b, $[Fe(CN)_6]^{4-}$ oxidation; peak c, $[Fe(CN)_6]^{3-}$ reduction).

(41) Kadirov, M. K.; Bosnjakovic, A.; Schlick, S. *J. Phys. Chem. B* **2005**, *109*, 7664−7670.
(42) Sando, G. M.; Dahl, K.; Owrutsky, J. C. *J. Phys. Chem. B* **2005**, *109*, 4084−4095.
(43) Brust, M.; Blass, P. M.; Bard, A. J. *Langmuir* **1997**, *13*, 5602−5607.

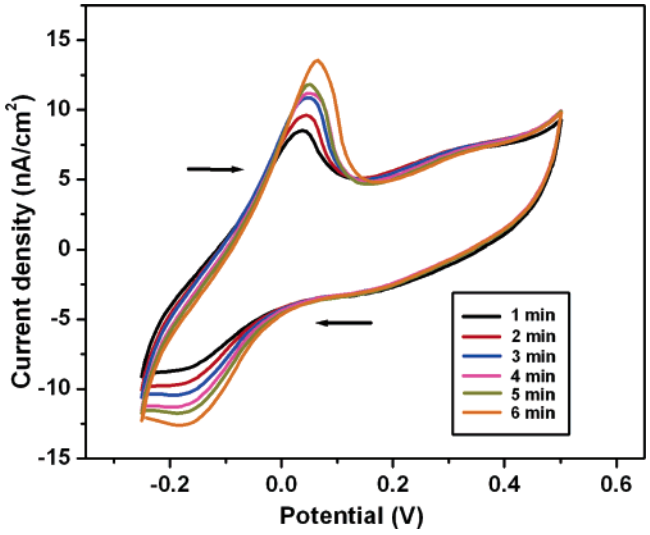

Figure 2. Hydrogen oxidation signal of the $K_4[Fe(CN)_6]$/Nafion membrane at a scan rate of 100 mV/s and scaling of the peak current with the partial pressure of H_2 (flow rate: 0.6 mL/min).

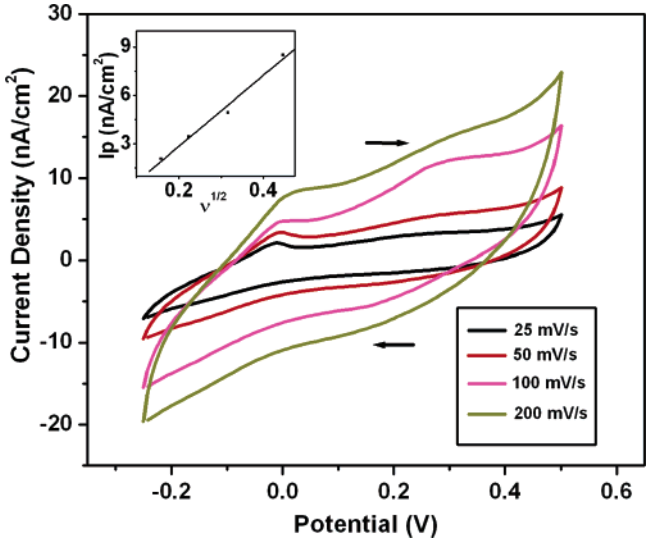

Figure 3. Cyclic voltammograms of the $K_4[Fe(CN)_6]$/Nafion membrane at different scan rates: (a) 25, (b) 50, (c) 100, and (d) 200 mV/s (inset: plot of $[Fe(CN)_6]^{4-}$ oxidation peak current (I_p) vs square root of scan rate ($n^{1/2}$) (V/s)).

mV when the scan rate is increased from 100 to 200 mV/s. Thus, using the above relationship, the anodic charge-transfer coefficient α for peak a is calculated to be 0.3. The peak current, I_p, of peak a as a function of the square root of scan rate (V/s) (inset, Figure 3) gives a straight line with a positive slope. An approximate calculation on the basis of the area under peak a yields a value of 1.48×10^{-2} mol/cm^3 for the concentration of protons in the $K_4[Fe(CN)_6]$/Nafion membrane. On the other hand, the reported values for pristine Nafion-film-modified electrodes dipped in aqueous electrolytes using Pt/RDE[32] and a Pt microelectrode[33] are 0.78×10^{-5} and 0.51×10^{-6} mol/cm^3 respectively. The values reported using film-modified electrodes are lower, maybe because of the exchange of protons in the film with the ions in the supporting electrolyte and maybe because of the presence of metal/film/solution triple phase boundary, which could contribute to the experimental parameters. Using the concentration of protons obtained by the above method and the slope of the I_p vs $\nu^{1/2}$ plot, we calculated the diffusion coefficient of protons in the ferrocyanide-incorporated solid electrolyte to be 4.8×10^{-12} cm^2/s using the expression for an irreversible electron-transfer process,[34] assuming diffusion as the principal mode of proton transport in Nafion

$$I_p = (2.99 \times 10^5)\alpha^{1/2} A D_o^{1/2} C_o^* \nu^{1/2} \quad (1)$$

where I_p is the peak current (A), α is the charge-transfer coefficient, A is the area of the working electrode (cm^2), D_o is the diffusion coefficient of the electroactive species (cm^2/s), C_o^* is the bulk concentration of protons (mol/cm^3), and ν is the scan rate (V/s). Thus the diffusion coefficient of protons in the ferrocyanide-incorporated Nafion membrane is found to be 7 orders of magnitude lower than that in 0.5 M H_2SO_4[35] (3.83×10^{-5} cm^2/s) and 2 orders of magnitude lower than that reported for the pristine Nafion membrane recast on a Pt electrode[32] (the permeability, $D_oC^*_o$, of protons is reported[32] as 1.2×10^{-11} mol cm^{-1} s^{-1}, from which the D_o expected for a proton concentration of 1.48×10^{-2} mol/cm^3 is calculated to be 8.57×10^{-10} cm^2/s). The decrease in the rate of proton diffusion in the present case implies a proton-coupled electron transfer for the $[Fe(CN)_6]^{4-}$/$[Fe(CN)_6]^{3-}$ couple. However, reports based on a molecular dynamics simulation[35] and a nonequilibrium statistical transport model[36] predict proton diffusion coefficients in the pristine Nafion membrane to be 5×10^{-6} and 1.9×10^{-5} cm^2/s, respectively. The observed discrepancy from the theoretical predictions could be because a Grotthus type diffusion mechanism[37] is assumed in both the reports, whereas in reality, more than one transport mechanism may be operating. The standard rate constant k^o for the oxidation of adsorbed hydrogen is calculated to be 9.06×10^{-6} cm/s using the expression for irreversible electron-transfer kinetics[34]

$$E_p = E_0' - RT/\alpha F[0.780 + \ln(D_o^{1/2}/k^o) + \ln(\alpha F\nu/RT)^{1/2}] \quad (2)$$

where, E_0' is the formal potential (−0.051V), ν is the scan rate (0.1 V/s), and E_p is the anodic peak potential (−0.003 V). From the standard rate constant, we found the exchange current density, j_o (defined as the exchange current (i_o) per

(44) Jacobs, P. A.; De Wilde, W.; Schoonheydt, R. A.; Uytterhoeven, J. B. *J. Chem. Soc., Faraday Trans.* **1976**, *72*, 1221
(45) Nicholson, R. S. *Anal. Chem.***1965**, *37*,11, 1351−1355.
(46) Kitamura, F.; Nanbu, N.; Ohsaka, T.; Tokuda, K. *J. Electroanal. Chem.* **1998,** *456*, 113−120.
(47) Dobson, K. D.; McQuillan, A. J. *Phys. Chem. Chem. Phys.* **2000**, *2*, 5180−5188.
(48) Binding energy values of the reference compounds were obtained from the NIST Web site, http://srdata.nist.gov/xps/bind_e_detail.
(49) *Handbook of X-Ray Photoelectron Spectroscopy*; Wagner, C. D., Riggs, W. M., Davis, L. E., Moulder, J. F., Mullenberg, G. E., Eds.; Perkin−Elmer: Wellesley, MA, 1979.
(50) Hush, N. S. *Electrochim. Acta* **1968**, *13*, 1005−1023.
(51) Glauser, M.; Hauser, U.; Herren, F.; Ludi, A.; Roder, P.; Schmidt, E.; Siegenthaler, H.; Wenk, F. *J. Am. Chem. Soc.* **1973**, *95*, 8457−8458.
(52) Khostariya, D. E.; Kjaer, A. M.; Marsagishvili, T. A.; Ulstrup, J. *J. Phys. Chem.* **1992**, *96*, 4154−4156.
(53) Details about sulfite oxidase are available on the Web site http://www.metallo.scripps.edu.
(54) Yeager, H. L; Steck, A. *J. Electrochem. Soc.* **1981**, *128*, 1880.
(55) Nafion structure based on the Yeager mode is available on the Web site http://www.psrc.usm.edu/mauritz/nafion.html.

unit area of the electrode), for hydrogen oxidation for the ion-incorporated membrane to be 6.8×10^{-6} A/cm^2 using the following expression[38]

$$i_o = nFAk^oC_o^*\exp[-\alpha f(E_{eq} - E_0')]$$

where i_o is the exchange current (A), n is the number of electrons involved in the redox process ($n = 1$ in this case), A is the area of the electrode (cm^2), k^o is the standard heterogeneous rate constant (cm/s), C_o^* is the bulk concentration of protons (mol/cm^3), α is the charge-transfer coefficient (0.3), $f = F/RT$ ($F = 96\,500$ C), E_{eq} is the equilibrium redox potential (0.164 V), and E_0' is the formal redox potential (-0.051 V).

The exchange current density thus calculated for hydrogen oxidation is found to be less by 3 orders of magnitude compared to that reported for the pristine Nafion membrane[32] (1.35×10^{-3} A/cm^2). However, the deviations in the calculated electrochemical parameters from the reported values could also be due to the inherent assumptions involved in the derivation of these expressions, as they were originally developed for liquid electrolytes. Nevertheless, they are broadly applicable for the treatment of solid electrolytes, except that they neglect additional modes of mass transport like migration and segmental mobility in the polymer matrix accompanying the mass transport of the incorporated species. Interestingly, the hydrogen oxidation peak becomes prominent only after the addition of potassium ferrocyanide to the Nafion membrane, which could be compared with a report on enhanced hydrogen sensitivity of the Nafion membrane by incorporation of chromium species.[39] This has important implications for designing electrocatalytic membrane-electrode assemblies (MEAs), wherein the rate of hydrogen oxidation could be modulated by using composite electrolytes. Also, this approach is quite different from the usual approach of using modified electrodes for electrocatalysis.

The origin of the quasi-reversible peaks b and c in Figure 1 could be easily attributed to the $[Fe(CN)_6]^{4-}/[Fe(CN)_6]^{3-}$ redox couple, because the peak currents increase with an increase in the concentration of potassium ferrocyanide. Whereas $[Fe(CN)_6]^{4-}/[Fe(CN)_6]^{3-}$ is a well-known reversible couple in aqueous electrolytes, it shows a quasi-reversible behavior (as is evident from the shift in peak separation (ΔE_p) with a change in the potential scan rate (Figure 3)) in the ionomer matrix because of the phase-separated structure of the polymer and its chemical interaction with the incorporated complex ions.

Furthermore, $K_3[Fe(CN)_6]$/Nafion (6.83×10^{-4} M) shows an open circuit potential of + 0.1 V, which is lower than that for the $K_4[Fe(CN)_6]$/Nafion membrane by 60 mV. This implies that $[Fe(CN)_6]^{3-}$ ions are more reducible in the Nafion environment than $[Fe(CN)_6]^{4-}$ ions. As a first sign of autoreduction, an anodic peak appears at +0.15 V in the first cycle on scanning the potential from its open circuit value in the anodic direction (Figure 4), which shows the presence of $[Fe(CN)_6]^{4-}$ species in the system. This observation is in excellent agreement with that reported by Murray et al. recently on the electron self-exchange dynamics of hexacyanoferrate, synthetically combined with a quarternary ammonium countercation connected to polyether chains to form redox hybrid molten salts.[40] This system is interestingly analogous to Nafion/hexacyanoferrate, except that the pendent chains have a charge opposite to that of the cyanoferrate ions. On the other hand, Schlick et al.[41] have reported the deleterious effect of Fe(III) ions on the stability of the Nafion membrane, wherein they have observed the formation of membrane-derived radical species arising because of the attack of ferric ions at the pendent chains in the ionomer. This could also be compared with a report by Sando et al.,[42] wherein the possibility of partial reduction of ferricyanide in anionic AOT (sodium bis(2-ethylhexyl) sulfosuccinate) micelles is mentioned, as well as with similar reports on the autoreduction of Cu^{2+} to Cu^+ on dithiol-modified copper electrodes[43] and the spontaneous reduction of Cu^{2+} in zeolites.[44]

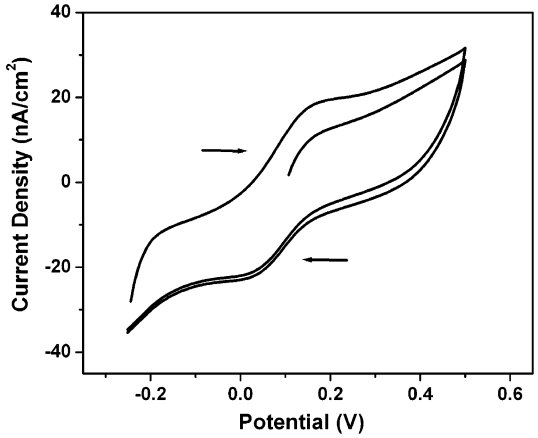

Figure 4. Cyclic voltammogram of the $K_3[Fe(CN)_6]$/Nafion membrane (6.83×10^{-4} M) at a scan rate of 100 mV/s when the potential is scanned in the anodic direction from the open circuit potential (0.1 V) to 0.5 V and then brought back to -0.25 V.

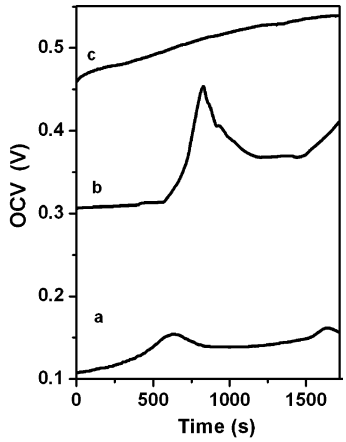

Figure 5. OCV vs time plots for $K_3[Fe(CN)_6]$/Nafion with different concentrations of ferricyanide: (a) 683, (b) 1366, and (c) 2732 μM.

3.1.2. Zero-Current Chronopotentiometry. The nature of open-circuit voltage versus time plots for the system (Figure 5) also reveals the instability of the $[Fe(CN)_6]^{3-}$ species in Nafion. Particularly interesting is the dependence of the OCV−time profiles on the concentration of the incorporated $[Fe(CN)_6]^{3-}$ ions, which provides a broader insight into the local structure of the ionomer that confines the redox species. Figure 5 shows the plots of OCV against time for Nafion membranes containing $K_3[Fe(CN)_6]$ at different concentra-

tions (683, 1366, and 2732 μM). It is found that at intermediate concentration (1.36×10^{-3} M), there is an exponential increase in OCV from 0.31 to 0.45 V for the first 13 min, after which it starts decreasing. The initial increase could be ascribed to the exchange of potassium ions with protons in the membrane and the later decrease signifies the autoreduction of $[Fe(CN)_6]^{3-}$ in the Nafion matrix. Also, the behavior changes with the concentration of $[Fe(CN)_6]^{3-}$, which might be due to the changes in the local structure of the micellar environment. On the other hand, at lower concentration (6.83×10^{-4} M), there is initially a slight increase in OCV, followed by a decrease (though the variation is only of the order of a few millivolts); at higher concentrations (2.73×10^{-3} M), a steady increase is noticed. A plausible explanation could be that in the former case, the anions present in the middle of the water pools enclosed by the sulfonate groups move to the interface between the hydrophilic and hydrophobic domains to get partially reduced, whereas in the latter case, the exchange of potassium ions of the redox species with the protons in the ionomer matrix could be the predominant process. This observed dependence of OCV on the concentration of the incorporated species reveals the micellar nature of the interface between the hydrophobic polymer backbone and the hydrophilic domains. However, there could be other contributions to the observed concentration dependence, such as the dynamics and segmental mobility of the polymer chains, which could accompany the mass transport of the redox species.

3.1.3. Electrochemical Impedance Studies. Panels a and b of Figure 6 show the Nyquist plots (Z(Im) vs Z(Re)) for the pristine Nafion membrane and the Nafion membrane containing equal amounts of potassium ferrocyanide and potassium ferricyanide (3.4×10^{-3} M in each), respectively. In the impedance plot of the modified membrane (Figure 6b), a curved portion is observed in the high-frequency region, whereas that of the unmodified membrane is almost linear (Figure 6a). This allows us to assign the curved portion in the modified membrane to the redox process of the complex species present in the polymer matrix; the linear region in the low-frequency part could be assigned to the mass transport of the species. The high-frequency part in Figure 6b is then fitted with a semicircle using the CNLS (complex nonlinear least-square fitting) method and fitting it with a simple Randles circuit. The resistance of the medium (R_s) is calculated to be 295 Ω/cm^2, and the charge-transfer resistance (R_{ct}) is found to be 6.15×10^3 Ω/cm^2. This yields a value of 5.66×10^{-6} cm/s for the rate constant, k^o, for $[Fe(CN)_6]^{4-}$ oxidation, from which the diffusion coefficient, D_o, of the complex anion is calculated to be 1.3×10^{-12} cm^2/s by adopting a treatment proposed by Nicholson[45] for quasi-reversible systems (assuming a value of 0.5 for the anodic charge-transfer coefficient, α). However, the standard expressions for deriving the electrochemical parameters were originally developed for liquid electrolytes, which could have some contribution to the deviation of the calculated values from those of the aqueous systems. The thermodynamic and kinetic parameters calculated for the $[Fe(CN)_6]^{4-}/[Fe(CN)_6]^{3-}$ couple and hydrogen oxidation in Nafion membrane are compiled in Table 1, which also provides a comparison with

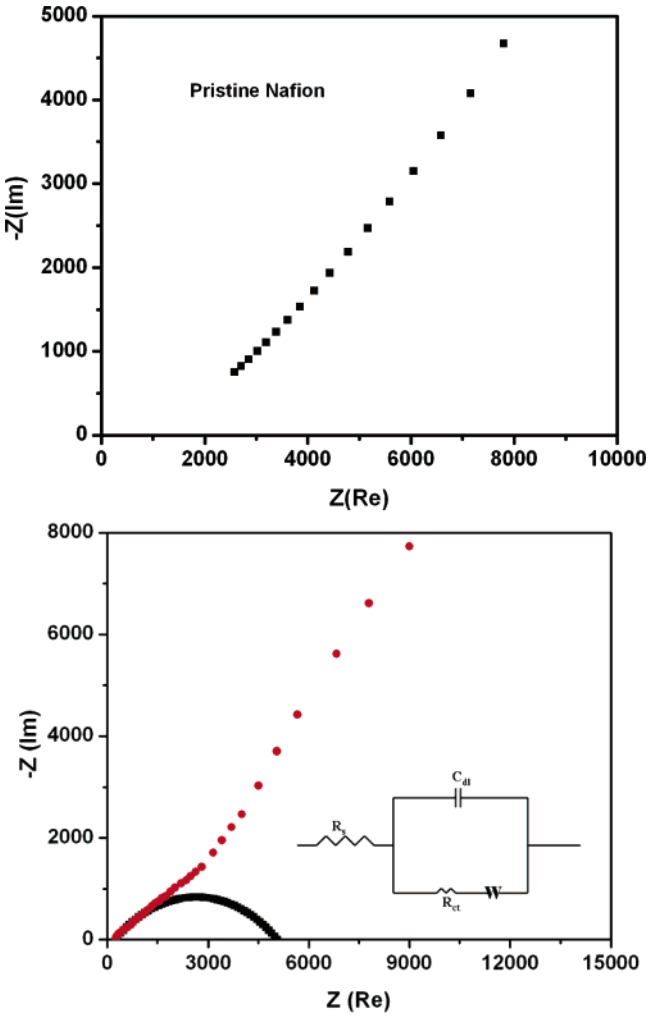

Figure 6. (a) Impedance plot of pristine (unmodified) Nafion membrane using a 10 mV Ac signal recorded in the frequency range 10 mHz to 100 kHz. (b) Impedance plot of the Nafion membrane containing equal amounts of $K_3[Fe(CN)_6]$ and $K_4[Fe(CN)_6]$ (3.4×10^{-3} M each) using a 10 mV rms AC signal in the frequency range 10 mHz to 100 kHz. (inset bottom right: equivalent circuit corresponding to the semicircle fitted with the high-frequency part).

Table 1. Thermodynamic and Kinetic Parameters Calculated from Electrochemical Experiments for $[Fe(CN)_6]^{4-}$ Oxidation and Hydrogen Oxidation in the Nafion Membrane

electrolyte	D_o (cm^2/s)	k^o (cm/s)	ΔG^o (kJ/mol)	α	j_o (A/cm^2)
Nafion[a]	1.3×10^{-12}	5.4×10^{-6}	−40.240	0.5	4.2×10^{-6}
0.5 M H_2SO_4[a]	4.7×10^{-6}	7.3×10^{-2}	−64.607	0.5	1.9×10^{-5}
Nafion[b]	4.8×10^{-12}	9.1×10^{-6}		0.3	6.7×10^{-6}

[a] $[Fe(CN)_6]^{4-}$ oxidation. [b] Hydrogen oxidation.

parameters in 0.5 M H_2SO_4 (obtained from electrochemical experiments performed simultaneously in our lab). Obviously, both charge transfer and mass transfer of ferrocyanide ions are more sluggish than those in aqueous electrolytes, as expected for a redox species incorporated in an unsupported solid electrolyte. For instance, the rate constant for $[Fe(CN)_6]^{4-}$ oxidation is found to be 4 orders of magnitude lower than that reported by Kitamura et al.[46] on Pt(100) in 0.5 M $KClO_4$ (4×10^{-2} cm/s) and the diffusion coefficient is lower by 6 orders of magnitude than the reported value[46] (6.32×10^{-6} cm^2/s). In comparison, Murray and co-workers[40] have observed a remarkable decrease in the diffusion coefficient (2.5×10^{-10} cm^2/s) by 4 orders of magnitude in

Table 2. Comparison of Binding Energies of Various Core Level Electrons in Cyanoferrate-Incorporated Nafion Membranes with Those in the Pristine Membrane along with BE Values Reported for Closely Related Systems.

core level	pristine Nafion (A/cm^2)	$K_4[Fe(CN)_6]$/Nafion (A/cm^2)	$K_3[Fe(CN)_6]$/Nafion (A/cm^2)	reported BE values (source)[a]
C 1s	284.6	283.8	285	284.8 (graphite)
C 1s	291.4	291.4	291.4	292.4 (Teflon)
O 1s	532.7	531.7	533.7	532.0 (RSO_3H)
O 1s	535.3	535.1	536.8	534.8 (entrapped water in polyamic acid)[b]
F 1s	688.9	689.0	690.5	690.0 (Teflon)
S 2p	169.8	168.8	170.7	169.0 ($F_3CSOOCH_3$)
Fe $2p_{3/2}$		708.5	710.1	709 ($K_4[Fe(CN)_6]$) 711 ($K_3[Fe(CN)_6]$)
N 1s		397.6	397.6	397.8 ($K_4[Fe(CN)_6]$)

[a] BE values reported in refs 38, 39 mentioned in the text. [b] This reference is given only to indicate the appearance of a separate O 1s peak for entrapped water molecules in polymer chains. However, in the discussion, the O 1s peak at lower binding energy is assigned to entrapped water molecules in Nafion based on the chemical environment, which is different from polyamic acid.

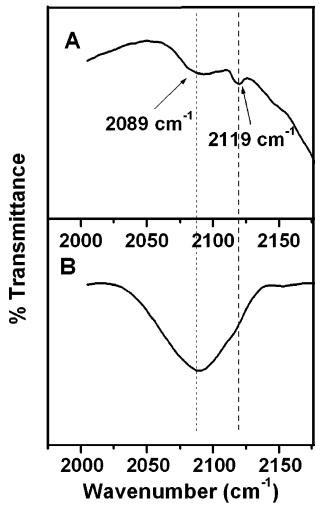

Figure 7. DRIFT spectra of (A) $K_3[Fe(CN)_6]$/Nafion and (B) $K_4[Fe(CN)_6]$/Nafion in the solid-state, recorded with a resolution of 4 cm^{-1}.

the redox polyether melt compared to that in aqueous solution (4×10^{-6} cm^2/s), which has been attributed to the dominance of electron hopping over the physical transport process. A further decrease by 2 orders of magnitude in the present system (1.3×10^{-12} cm^2/s) could be ascribed to a proton-coupled electron-transport mechanism because of its similarity to the proton diffusion coefficient (4.8×10^{-12} cm^2/s) calculated above. However, while deriving kinetic parameters from aqueous solutions, complications arising from adsorption of the redox species on the electrode surface leading to an innersphere mechanism must also be considered, as reported by Kitamura et al.[46] In this context, a polymer electrolyte/redox hybrid is one the most promising systems for evaluating pure outersphere electron-transfer processes without any complications from adsorption.

These observations demonstrate the possibility for predicting the charge-transfer and mass-transfer dynamics in catalyst-coated membranes—an alternate technology useful in fuel cells, wherein the catalyst material is coated directly on the polymer electrolyte membrane, instead of coating over the electrodes.

3.2. Spectroscopic Investigations. *3.2.1. DRIFT Spectroscopy.* Figure 7 shows the Fourier transform infrared spectra (in diffuse reflectance mode) of the $K_3[Fe(CN)_6]$/Nafion membrane (Figure 7A) and the $K_4[Fe(CN)_6]$/Nafion membrane (Figure 7B). Compared to the ν_{CNstr} for aqueous solutions of potassium ferrocyanide[47] (2037 cm^{-1}) and ferricyanide (2115 cm^{-1}), those in the Nafion membrane (2090 cm^{-1} and 2122 cm^{-1}, respectively) show a slight blue shift. The increase in the CN bond energy in the latter case implies an increase in the metal-to-ligand $\pi-\sigma^*$ back-bonding, which in turn could be due to an increase in electron density at the metal center. This could be possible if the pendent sulfonate groups of the polymer interact with the iron center to form a partial bond, thereby increasing the electron density in the vacant d orbitals of the metal. Such interactions play a crucial role in deciding the charge-transfer dynamics and energetics of the redox couple in the polymer matrix. Interestingly, the $K_3[Fe(CN)_6]$/Nafion membrane shows absorption at frequencies corresponding to the ν_{CNstr} of both cyanoferrate(III) and cyanoferrate(II) (2122 cm^{-1} and 2090 cm^{-1}, respectively), whereas the $K_4[Fe(CN)_6]$/Nafion membrane shows no signature of cyanoferrate(III) after CV. Thus the autoreduction of ferricyanide to ferrocyanide in the Nafion matrix is evident from the above results from DRIFT spectroscopy.

3.2.2. X-ray Photoelectron Spectroscopy. Figure 8 shows the O 1s, S 2p, and Fe 2p core level XP spectra of Nafion membranes containing potassium ferricyanide (Figure 8A) and potassium ferrocyanide (Figure 8B), along with the O 1s and S 2p spectra of the pristine membrane (Figure 8C). In all the cases, two peaks are observed in the O 1s spectra, of which the peak appearing at higher BE could be attributed to the oxygen in the sulfonic acid group and the other component at a lower BE is due to the entrapped water molecules.[48] An increase in the BE of sulfonate oxygen (by 1.5 eV) observed in ferricyanide-containing Nafion compared to that of the pristine membrane could be due to the ligation of sulfonate oxygen to the iron center in the ferricyanide ion, thereby facilitating the reduction of the latter. On the other hand, no such increase in BE is observed after the addition of ferrocyanide ions. Similarly, an increase in BE is observed for the S 2p level, confirming the validity of the explanation given above for the BE shift for O 1s level. The Fe 2p region of the $K_4[Fe(CN)_6]$/Nafion membrane shows a main Fe $2p_{3/2}$ peak at 708.5 eV and associated satellites at 714 eV as expected for $[Fe(CN)_6]^{4-}$. On the other hand, the Fe 2p spectrum of the $K_3[Fe(CN)_6]$/Nafion membrane shows a Fe $2p_{3/2}$ peak at 710.1 eV, which is intermediate between the BE values expected for pure $K_4[Fe(CN)_6]$ (708−709 eV) and $K_3[Fe(CN)_6]$ (711 eV).[48,49] This shows the presence of

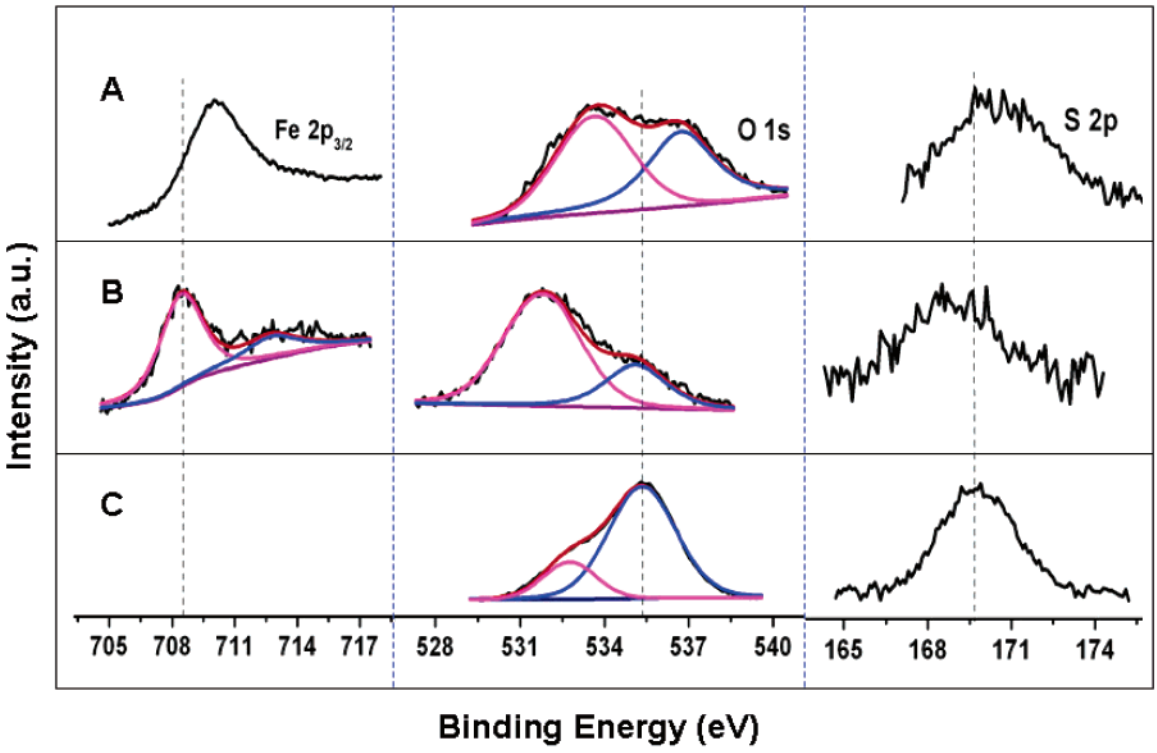

Figure 8. Fe 2p, S 2p, and O 1s XP spectra of (A) $K_3[Fe(CN)_6]$/Nafion and (B) $K_4[Fe(CN)_6]$/Nafion, and (C) S 2p, O 1s XP spectra of the pristine Nafion membrane (black lines show plots of raw data; colored lines show fitted data (wherever necessary) using a combined polynomial and Shirley type background function).

a mixture of ferric and ferrous species that would have been formed during the autoreduction of potassium ferricyanide in Nafion matrix. Also, no $[Fe(CN)_6]^{3-}$ peak appears for the $K_4[Fe(CN)_6]$/Nafion after cyclic voltammetry. The experimental BE values for C 1s, F 1s, and N 1s core levels are found to be in close agreement with the reported values, which are compiled in Table 2.

Thus the above XPS investigations clearly demonstrate the autoreduction of $[Fe(CN)_6]^{3-}$ in the Nafion environment, mediated by the oxidation of sulfonate groups.

3.2.3. ESR Spectroscopy. Cyanoferrates belong to the class of low-spin metal complexes. In the native state, ferrocyanide is diamagnetic and ferricyanide is paramagnetic. Hence the $[Fe(CN)_6]^{3-}$/Nafion system is expected to be amenable for ESR studies. Surprisingly, this material is found to be ESR-silent in the magnetic field region of 500−6500 G, which also overs the region of the expected peaks at $g = 4$, indicating in agreement with the other characterization studies that the Fe center is reduced from the +3 to +2 state when present in the Nafion matrix.

3.2.4. UV−Visible Spectroscopy. Figure 9 shows the UV−visible spectra of cyanoferrate(II) (Figure 9B) and cyanoferrate(III) (Figure 9C) along with that of the cyanoferrate(III)-incorporated Nafion membrane (Figure 9A) (6.7×10^{-3} M), all recorded in the solid state. In the UV−visible spectrum of the $VK_3[Fe(CN)_6]$-incorporated Nafion membrane, broad bands are seen at 247 and 296 nm, which are intermediate between the corresponding bands observed for $K_4[Fe(CN)_6]$ (239 and 275 nm) and $K_3[Fe(CN)_6]$ (258 and 298 nm), respectively. This is an obvious indication of the presence of both species in the membrane in which only ferricyanide was added initially. Also, it is worth mentioning here that

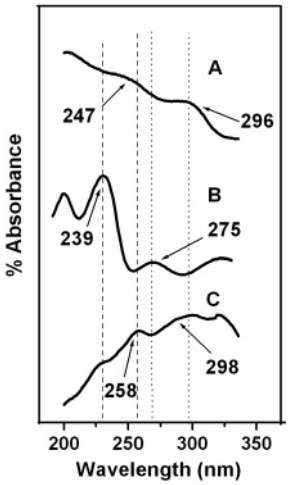

Figure 9. UV−visible spectra of (A) $K_3[Fe(CN)_6]$/Nafion, (B) $K_4[Fe(CN)_6]$, and (C) $K_3[Fe(CN)_6]$ recorded in the solid state.

the possibility of the formation of mixed-valence polynuclear complexes is very low at such low concentrations used in this study.[50−52]

3.3. Mechanism of $[Fe(CN)_6]^{3-}$ Autoreduction. On the basis of the above observations, a possible mechanism is proposed for the interaction of $K_3[Fe(CN)_6]$ with Nafion and its subsequent autoreduction (Scheme 2). The first step in the proposed mechanism is the exchange of potassium ions with protons in the sulfonate groups of the ionomer. This is supported by the observed decrease in the OCV of the pristine Nafion membrane by 116 mV after the addition of potassium ferrocyanide. Also, the concentration-dependent OCV−time plots indicate that the complex ion initially in the middle of the water pool moves to the micellar interface,

Scheme 2. Mechanism of $[Fe(CN)_6]^{3-}$ Autoreduction in the Nafion Membrane

1) **Proton Exchange:**

$$K_3[Fe(CN)_6] + x\ RSO_3^-H^+ \longrightarrow K_{3-x}H_x[Fe(CN)_6] + x\ RSO_3^-K^+$$

2) **Autoreduction:**

$$[Fe(CN)_6]^{3-} + RSO_3^- \longrightarrow [Fe(CN)_6]^{4-} + RSO_3^{\cdot}$$

where the potassium ions are exchanged with the protons in the membrane, followed by its autoreduction. Subsequent to this initial cation exchange, the sulfonate groups (where S is in the +4 state) are found to ligate (through the oxygen atom) to the iron center and facilitate reduction of $[Fe(CN)_6]^{3-}$ to $[Fe(CN)_6]^{4-}$, themselves getting oxidized, probably to sulfonate radical, as reported by Schlick et al., wherein the attack of Fe(III) species on the sulfonate pendent groups in Nafion produces membrane-derived radical species.[41] The initial ligation of sulfonate oxygen to the iron center is evident from the increase in the O 1s BE value of sulfonate oxygen on addition of ferricyanide to the polymer. In the case of ferrocyanide-containing Nafion, such a shift is not observed, which is expected in light of the theory of hard and soft acids and bases (HSAB), because sulfonate oxygen would interact more strongly with the Fe(III) center than with Fe(II). It is very exciting to note that a similar mechanism already exists in biological systems, wherein ferricytochrome C acts as the final electron acceptor in the oxidation of sulfite ions catalyzed by sulfite oxidase enzyme present in the mitochondria of human cells.[53]

Thus a reasonable understanding of the interactions of the incorporated ions with polymer electrolytes at the molecular level could be attained by a judicious combination of complementary techniques, as demonstrated in this work. This property of the polymer electrolyte is broadly analogous (despite different mechanisms) to the role of the CeO_2 component in the solid electrolyte (CeO_2/ZrO_2) for solid oxide fuel cells, wherein CeO_2 provides a better dispersion of the catalyst by tuning its redox potential, thereby enhancing the activity of the incorporated catalyst. This incorporated ion probe protocol may also provide valuable insights into the mechanism of membrane degradation caused by impurity-generated radical intermediates under the operating conditions of fuel cells.

4. Summary and Conclusions

The above investigations demonstrate the inherent capability of the Nafion membrane to tune the redox potential of the incorporated ions in addition to proton conduction, unlike the electrode potential-induced redox properties of Nafion reported earlier. The similarity of the diffusion coefficient (obtained from the electrochemical data) of $[Fe(CN)_6]^{4-}$ incorporated in the Nafion membrane to that of protons allows us to surmise a proton-coupled electron-transfer mechanism for the $[Fe(CN)_6]^{4-}/[Fe(CN)_6]^{3-}$ couple. Also, the dependence of OCV−time profiles on the concentration of ferricyanide ions incorporated in the membrane reveals the micellar nature of the interface between the hydrophilic and hydrophobic domains in the polymer. Thus the cyanoferrate anions incorporated in the anionic resin are demonstrated to serve as effective probes in unfolding the structural, thermodynamic, and charge-transport pathways of the ionomer. These results could be applied in the fabrication of catalyst-coated membranes, for choosing the proper form of the catalyst material having redox compatibility with the ionomer and in deciding their relative proportions to achieve optimum efficiency in fuel cells and supercapacitors. In addition to that, the hydrogen oxidation signal observed in the CV of the $K_4[Fe(CN)_6]$/Nafion membrane has direct implications for fuel cells, as an anodic process in H_2/O_2 PEFCs as well as in solid-state hydrogen sensing, because the peak current scales with hydrogen concentration.

Acknowledgment. M.P. acknowledges the Council of Scientific and Industrial Research, New Delhi, India, for providing a Junior Research Fellowship. We are thankful to Dr. D. Srinivas for his valuable suggestions and excellent discussions. We are also thankful to Dr. B. L. V. Prasad, NCL, for providing the IR and UV−vis facility and Dr. P. Manikandan for providing the solid-state UV−vis facility. We also thank Dr. Sivaram, Director, National Chemical Laboratory, for his constant encouragement and support.

CM061444I